HHS Public Access

Author manuscript

Neuron. Author manuscript; available in PMC 2017 December 14.

Published in final edited form as:

Neuron. 2017 November 15; 96(4): 897–909.e5. doi:10.1016/j.neuron.2017.09.042.

Enhanced AMPA receptor trafficking mediates the anorexigenic effect of endogenous glucagon like peptide-1 in the paraventricular hypothalamus

Ji Liu[1,2], **Kristie Conde**[1,2], **Peng Zhang**[3], **Varoth Lilascharoen**[4], **Zihui Xu**[1,2], **Byung Kook Lim**[4], **Randy J. Seeley**[5], **Julius J. Zhu**[3], **Michael M. Scott**[3,*], and **Zhiping P. Pang**[1,2,6,*]

[1]Child Health Institute of New Jersey, Rutgers University Robert Wood Johnson Medical School, New Brunswick, New Jersey, 08901, USA

[2]Department of Neuroscience and Cell Biology, Rutgers University Robert Wood Johnson Medical School, New Brunswick, New Jersey, 08901, USA

[3]Department of Pharmacology, University of Virginia, Charlottesville, Virginia, 22908, USA

[4]Department of Neurobiology, University of California San Diego, California, 92093, USA

[5]Department of Surgery, University of Michigan, Ann Arbor, Michigan, 48109, USA

SUMMARY

Glucagon Like Peptide 1 (GLP-1)-expressing neurons in the hindbrain send robust projections to the paraventricular nucleus of the hypothalamus (PVN), which is involved in the regulation of food intake. Here, we describe that stimulation of GLP-1 afferent fibers within the PVN is sufficient to suppress food intake independent of glutamate release. We also show that GLP-1 receptor (GLP-1R) activation augments excitatory synaptic strength in PVN corticotropin-releasing hormone (CRH) neurons, with GLP-1R activation promoting a protein kinase A (PKA) dependent signaling cascade leading to phosphorylation of serine S845 on GluA1 AMPA receptors and their trafficking to the plasma membrane. Finally, we show that postnatal depletion of GLP-1R in the PVN increases food intake and causes obesity. This study provides a comprehensive multi-level (circuit, synaptic, and molecular) explanation of how food intake behavior and body weight are regulated by endogenous central GLP-1.

Keywords

GLP-1; paraventricular hypothalamus; AMPA receptor; synaptic transmission; phosphorylation; membrane trafficking; electrophysiology; feeding; food intake behavior; obesity

[*]Correspondence: Zhiping P. Pang, Ph.D., zhiping.pang@rutgers.edu, Child Health Institute of New Jersey, Rutgers University, 89 French Street, New Brunswick, NJ 08901, USA, Lead contact for: Ji Liu, Kristie Conde, Zihui Xu, Varoth Lilascharoen, Byung Kook Lim and Randy Seeley or Michael M. Scott Ph.D., michael.scott@virginia.edu, 1340 Jefferson Park Ave. Jordan Hall, Charlottesville, VA 22908, USA, Lead contact for: Peng Zhang and Julius J. Zhu.

[6]Lead author

Author contribution:

Z.P.P. and J.L. conceived the project and designed the experiments. J.L. performed all experiments and analyzed the data. K.C. and Z.X performed behavior tests. P.Z, and JJ Zhu provided the Sindbis viruses for expressing GluA1-Ct and GFP; B.K.L provided retrograde tracing rabies viruses, R.S. provided GLP-1 floxed mice; M.S. provided the *Gcg-Cre* mouse line. J.L and Z.P.P. wrote the paper. All authors provided intellectual contribution towards writing of the manuscript.

INTRODUCTION

Glucagon like peptide 1 (GLP-1), an incretin hormone and a post-translational cleavage product of preproglucagon encoded by the *Gcg* gene, is mainly produced in the L-cells of the intestine and in a subpopulation of hindbrain Nucleus Tractus Solitarius (NTS) neurons (Holst, 2007; Larsen et al., 1997). In the central nervous system (CNS), GLP-1R agonist administration suppresses feeding and reduces body weight (McMahon and Wellman, 1998; Mietlicki-Baase et al., 2013; Secher et al., 2014; Turton et al., 1996), but how central endogenous GLP-1 is involved in feeding control is even less understood.

The NTS GLP-1 producing neurons send robust projections to many forebrain regions, including the paraventricular nucleus of the hypothalamus (PVN) (Gaykema et al., 2017; Gu et al., 2013). The PVN is one of several brain centers implicated in food intake behavior (Betley et al., 2013), as lesioning of the PVN induces overeating and obesity (Shor-Posner et al., 1985; Sims and Lorden, 1986). PVN contains diverse cell types, including corticotropin releasing hormone (CRH)-, oxytocin (Oxt)-, and arginine vasopressin (AVP)-expressing neurons, which likely contribute to feeding behavior regulation (Hotta et al., 1991; Olson et al., 1991; Sutton et al., 2014). Moreover, PVN neurons express GLP-1R (Cork et al., 2015), and direct infusion of GLP-1 into the PVN suppresses food intake (McMahon and Wellman, 1998), while GLP-1 antagonists increase food intake (Katsurada et al., 2014). However, a recent study suggests that conditional ablation of GLP-1R expression in Sim-1 neurons of mice shows minimal effects on food intake (Ghosal et al., 2017), which is inconsistent with previous pharmacological studies (Katsurada et al., 2014; McMahon and Wellman, 1998). This is likely due to 1) the difference between endogenous GLP-1 and exogenous GLP-1 agonist function, or due to the fact that 2) since GCG neurons are also proposed to co-release glutamate (Zheng et al., 2015), GLP-1 peptide signaling is redundant or, finally, 3) that alternate neuronal pathways can compensate for the loss of GLP-1Rs, following early developmental deletion from Sim1 neurons (Fan et al., 1996). Thus, it is crucial to understand how endogenous GLP-1 acts on PVN neurons to regulate feeding behavior, and whether the GLP-1 signal is sufficient and necessary to control food intake.

In addition to a lack of understanding of whether GLP-1 release at a specific CNS target is necessary or sufficient to affect food intake, it is also unclear how GLP-1 modulates the activity of the postsynaptic target. The specific signaling cascades post-GLP-1R activation likely vary depending on how G proteins ($G\alpha_s$, $G\alpha_$, $G\alpha_q$ and $G\alpha_{i/o}$) selectively couple with the GLP-1 receptor (Hallbrink et al., 2001; Montrose-Rafizadeh et al., 1999). For example, in the peripheral pancreatic islets, GLP-1 activates adenylate cyclases, increases cAMP levels, and activates the PKA/Epac2 pathway, increasing the influx of Ca^{2+} and inhibition of Kv channels (Drucker et al., 1987; Montrose-Rafizadeh et al., 1999; Thorens, 1992; Wheeler et al., 1993). In the hypothalamus, meanwhile, GLP-1R signaling may facilitate excitatory presynaptic release (Acuna-Goycolea and van den Pol, 2004) and increase presynaptic vesicle release probability in the mesolimbic dopamine system (Mietlicki-Baase et al., 2014). However, the intracellular signaling cascades activated by GLP-1 in the PVN have not been described.

To address these outstanding questions described above, in the present study, we use a recently generated *Gcg-Cre* recombinase BAC transgenic mouse line (Gaykema et al., 2017), which provides a unique tool for specifically investigating functions of NTS GCG neurons using optogenetic and chemogenetic approaches. We address the functional anatomical impact of the NTS-to-PVN projecting neural pathway and show that GLP-1 signaling is sufficient to suppress feeding independent of glutamate co-release from GCG neurons. By using slice physiology, we show that GLP-1R activation specifically increases the excitatory, but not inhibitory, synaptic strength to CRH neurons through an enhancement of AMPA receptor (AMPAR) subunit membrane trafficking. Furthermore, we also show that phosphorylation of amino acid S845 on the C-terminus of GluA1 is involved in augmenting the postsynaptic surface expression of this AMPAR subunit. Finally, we find that postnatal ablation of PVN GLP-1R causes an increase in food intake, body weight gain and obesity, suggesting the necessity of GLP-1R signaling in the regulation of body weight homeostasis. These data elucidate the structural and molecular basis of how endogenous GLP-1 functions in the brain to control food intake and body weight.

RESULTS

NTS–to–PVN GLP-1 projection targets CRH neurons

To investigate the function of endogenously released GLP-1 in the brain, we used *Gcg-Cre* (GLP-1 is a post-translational cleavage product of *Gcg* encoded preproglucagon protein) transgenic animals that we recently generated and carefully characterized (Gaykema et al., 2017). We first asked whether PVN neuronal activity is modulated by the activity of NTS GLP-1 producing GCG neurons. Adeno-associated viruses (AAVs) harboring DIO-hM_3Dq-mCherry, a Cre-dependent stimulatory Designer Receptor Exclusively Activated by Designer Drugs (DREADDs) and Cre-dependent YFP were injected into the NTS and the PVN region respectively of *Gcg:CRH-Cre* double transgenic mice. Administration of the DREADD ligand Clozapine-N-oxide (CNO) by intraperitoneal (i.p.) injection significantly increased c-Fos protein expression in the PVN CRH neurons (labeled by YFP, Figure 1A to D), suggesting that CRH neuronal activity can be driven by activation of NTS GCG neurons. Interestingly, the application of Exendin-9 (Exn9), a specific GLP-1R antagonist (Turton et al., 1996), blocked GCG neuronal activation-induced c-Fos expression in the PVN (Figure S1A&B), suggesting an involvement of GLP-1R signaling in NTS-to-PVN neural pathways. However, these results do not address whether the activation of CRH neurons initiated by GLP-1 is via direct or indirect GLP-1R activation.

To address this question, we first asked whether PVN CRH neurons express GLP-1R. We took advantage of Fluorescein-Trp^{25} – Exendin-4 (F-Exn4), which has been shown to have a similar anorexic effect as Exn4 at the same dose (Rajan et al., 2015; Reiner et al., 2016), and is a high affinity ligand of GLP-1R. We incubated live hypothalamic brain slices for 15 min in artificial cerebrospinal fluid (ACSF) with 100 nM F-Exn4 before fixing the tissue and performing immunohistochemistry (IHC). We found that F-Exn4 labeled live neurons can be readily identified after fixation, with most expressing CRH while some were also found to express Oxt, but none were found to express AVP (Figure S2A, C&E). Importantly, F-Exn4 did not bind to CRH or Oxt neurons when GLP-1Rs were ablated genetically, which was

achieved by crossing *CRH-* or *Oxt-Ires-Cre* mice with floxed GLP-1R (*GLP-1R*$^{f/f}$) mice (Sisley et al., 2014), demonstrating the specificity of the assay (Figure S2B&D).

Next, we asked whether NTS GCG neurons form direct synaptic contacts with CRH neurons. Taking advantage of Channelrhodopsin 2 (ChR2) -assisted circuit mapping (CRACM), we injected the Cre-dependent AAV expression vectors ChR2-YFP and tdTomato into the NTS and PVN, respectively, of *Gcg:CRH-Cre* transgenic mice. The *ex vivo* electrophysiologic assessment of light-evoked postsynaptic currents in downstream neurons was then performed in acute hypothalamic brain slices (Figure 1E). We found many GCG (i.e. GLP-1) fibers were located in close proximity to the CRH neurons in the PVN (Figure 1F). Strikingly, blue light evoked EPSCs were detected in more than half of the CRH neurons, while only 5 out of 23 non-CRH neurons responded to the GCG stimulation input (Figure 1G, H&I). Since NTS GCG neurons also express vesicular glutamate transporter Vglut2 (Zheng et al., 2015), deletion of Vglut2 would be expected to abolish the release of glutamate in GCG neurons. We thus generated the *Gcg-Vglut2 knockout (KO)* using the *Gcg-Cre* and the floxed *Vglut2* (*Vglut2*$^{f/f}$) mice (Tong et al., 2007), and found that light evoked glutamate release from the GCG nerve terminal in the PVN was abolished (Figure 1G&I). The CRACM results clearly show the direct synaptic contact between GCG and CRH neurons. To further confirm this pathway, we used a modified rabies virus $SAD_{\Delta}G$ –EGFP (EnvA-$SAD_{\Delta}G$-EGFP) in combination with Cre-dependent helper AAVs expressing TVA (receptor for the avian sarcoma leucosis virus glycoprotein EnvA; AAV-DIO-tdTomato-TVA) and RG (rabies envelope glycoprotein; AAV-DIO-RV-G) injected into *Gcg:CRH* double-*Cre* transgenic animals. AAV-DIO-tdTomato-TVA and AAV-DIO-RV-G were injected into the PVN, allowing rabies infection of CRH neurons and subsequent retrograde trans-synaptic spread. Three weeks post-AAV transduction, we injected $SAD_{\Delta}G$ –EGFP into the same area to infect CRH neurons. One week prior to $SAD_{\Delta}G$ –EGFP injection, the Cre-dependent expression of mCherry (AAV-DIO-mCherry) was injected into the NTS to label GLP-1 expressing neurons (Figure 1J). GFP positive cells projecting to PVN CRH neurons were found in the NTS area and half of them were also mCherry positive, indicating expression of *Gcg-Cre* recombinase (Figure 1K&L).

Taken together, these data suggested that NTS GLP-1 producing neurons directly project to the PVN CRH neurons, yielding neuronal excitation.

NTS–to–PVN GLP-1 signaling is sufficient to suppress food intake

We hypothesized that targeted activation of NTS-to-PVN projections would affect feeding behavior in mice. To address this question, Cre-activated AAV-ChR2-YFP (DIO-ChR2-YFP) was injected into the NTS region of *Gcg-Cre* transgenic mice. To specifically activate GCG terminals within the PVN *in vivo*, optical fibers were implanted into the PVN region bilaterally (Figure 1M). Optical stimulation of GCG nerve terminals within the PVN resulted in a reduction in food intake for the duration of the stimulation in animals with restricted overnight food consumption (Figure 1N). This suggests that the activation of the NTS-to-PVN projections is sufficient to suppress acute food intake. We further confirmed our observations by bilaterally injecting CNO into the PVN of hM_3Dq expressing *Gcg-Cre* animals (Figure S1 C&D) to activate the GCG nerve terminals within the PVN

chemogenetically. Importantly, Exn9, a specific blocker for GLP-1R, completely blunted the suppressive effects observed with activation of NTS-to-PVN projections (Figure S1E), suggesting the GLP-1R signal activation within the PVN is crucial to the function of GCG neurons centrally in the regulation of feeding behavior. Conversely, using DIO-eArch3.0-EYFP expressed in NTS GCG neurons to optogenetically inhibit GCG terminals in the PVN, we observed an increased in food intake in non-food restricted *Gcg-Cre* animals (Figure 1O). Together, our data suggests that NTS-to-PVN GLP-1 neural pathway is critical for central control of food intake.

Thus far, we have shown how CRH neurons in the PVN receive synaptic inputs and are regulated by NTS GCG neurons. We therefore hypothesized that PVN CRH neurons may be involved in the GLP-1-dependent regulation of food intake. However, a previous study showed that CRH neurons might not be necessary to regulate appetite, as chemogenetic inhibition of these neurons did not affect food intake (Garfield et al., 2015), a finding which we have confirmed (Figure S1, F&G). However, as stimulation of PVN CRH neurons slightly but significantly suppressed food intake by i.p. injection of CNO to hM_3Dq infected *CRH-Cre* mice (Figure S1, H&I), we then examined the necessity of CRH activation in the GLP-1 dependent regulation of food intake in the PVN. We injected AAV-DIO-ChR2 and AAV-DIO-hM_4Di into the NTS and PVN, respectively, in *Gcg:CRH-Cre* transgenic animals. Prior to blue light stimulation, CNO was i.p. delivered to block CRH neuronal activity via hM_4Di (Figure 1P). We found that ChR2-evoked suppression of food intake (Figure 1M&N) was at least partly blocked by inhibiting CRH neurons chemogenetically (Figure 1P&Q). Therefore, CRH neuronal activation in the PVN by GLP-1 likely contributes to suppression of food intake.

It has been suggested that GCG neurons also release glutamate in the PVN (Figure 1G–I), and it is of interest to elucidate whether glutamate release in the NTS-PVN pathway may also mediate food intake regulation. We thus crossed the *Gcg-Cre* mice with floxed *Vglut2* (*Vglut2*$^{f/f}$) animals to obtain the Gcg-neuronal specific Vglut2 KO. *Gcg-Vglut2 KO* mice showed normal body weight and daily energy consumption compared to control animals (Figure S1, J–L). Remarkably, when we utilized photostimulation of GCG neuronal terminal within the PVN, the *Gcg-Vglut2* KO animals showed the exact same pattern of feeding (suppression of food intake when compared with control animals) as *Gcg-Cre* animals (Figure 1N). This suggests that the NTS GCG to PVN projection is sufficient to suppress food intake and this effect is likely independent of local glutamate release.

Augmentation of excitatory synaptic strength in PVN CRH neurons by GLP-1 signaling

To investigate the cellular mechanisms underlying the GLP-1 mediated excitation of PVN CRH neurons, we focused on elucidating the synaptic mechanism. Exnedin-4 (Exn4), a specific GLP-1R agonist (Thorens et al., 1993), significantly increased the amplitude of spontaneous excitatory postsynaptic currents (sEPSC) in CRH neurons, while the frequency was not changed (Figure 2A&D, Figure S3A). We next examined miniature EPSCs (mEPSCs) in the presence of tetrodotoxin (TTX). Remarkably, similar to sEPSCs, we also found a significant increase of mEPSC amplitude, but not frequency, after the application of Exn4 (Figures 2B&E, and Figure S3B). Importantly, the effect of GLP-1 on mEPSCs in

PVN CRH neurons was abolished by ablation of GLP-1R in this cell type, which indicates the activation of CRH neurons is indeed directly mediated by the GLP-1R signaling cascade (Figures 2C&F). Neither amplitude nor frequency of the spontaneous inhibitory postsynaptic currents (sIPSCs) was altered by GLP-1R activation (Figures S3E–G), which indicates that the excitatory tone is selectively targeted by GLP-1R signaling within the PVN.

An increase in quantal size (i.e. mEPSC amplitude) can be a result of either an increase in presynaptic vesicle content or an increase in postsynaptic glutamatergic AMPARs. Given the expression of GLP-1R in the PVN CRH neurons (Figure S2), we hypothesized that a postsynaptic mechanism mediates the GLP-1 regulation on synaptic transmission. To this end, we recorded evoked EPSCs in the PVN CRH neurons using local electric stimulation in the absence or presence of Exn4. We analyzed the ratio of AMPA/NMDA receptor mediated evoked EPSCs and found it was dramatically increased after application of Exn4 (Figures 2G&H). These data provide strong evidence that GLP-1 enhances excitatory synaptic transmission postsynaptically, likely via facilitating the trafficking of AMPARs to the membrane (Citri and Malenka, 2008). Meanwhile, no change in the paired-pulse ratio (PPR) was found in the presence of Exn4, suggesting an increase in presynaptic release is not involved (Figure S3, C&D). These data further strengthen the conclusion that GLP-1 signaling in the PVN facilitates CRH neuronal excitatory inputs via postsynaptic modifications of the PVN neuron. Additionally, we found that the fraction of PVN Oxt neurons that responded to GLP-1 also showed a similar response to Exn4 as compared to CRH neurons (Figure S3, H–M). This is consistent with the *in vitro* F-Exn4 binding experiment, which showed a small portion of Oxt neurons might express GLP-1R (Figure S2C).

It has been shown that GluA1 subunits are inserted into the postsynaptic membrane during the early phase of long-term synaptic potentiation, potentially forming GluA2-lacking AMPARs that demonstrate rectification (Takahashi et al., 2003). Thus the rectification index measured by the ratio of AMPAR mediated EPSC amplitudes recorded at +40 mV holding potential vs. amplitudes recorded at −70 mV holding potential has been used as an indication of AMPAR membrane trafficking (Takahashi et al., 2003). We recorded evoked EPSCs in the presence of D-APV and picrotoxin at different holding potentials with an internal solution containing 100μM spermine, and calculated the rectification index, which showed an increase in the presence of Exn4 (Figure 2I&J), suggesting GluA2-lacking AMPARs are involved in mediating the stimulatory effects of GLP-1R activation. To substantiate this, we applied IEM1460, a specific GluA2 lacking, Ca^{2+} permeable, AMPAR blocker prior to the application of Exn4, which completely blocked the augmentation effect of Exn4 (Figure 2K&L). Taken together, we propose that the post-synaptic augmentation of GLP-1R signaling in CRH neurons is likely mediated by the increased membrane trafficking of GluA1.

To further test the hypothesis that GluA1 membrane recruitment is involved in GLP-1R signaling, we sought to examine the impact of blocking GluA1 trafficking. Given that expression of the cytoplasmic termini (CT) of GluA1 has been previously shown to block trafficking of endogenous GluA1 in a dominant negative manner (McCormack et al., 2006), we infected PVN neurons with sindbis viruses expressing either GluA1-CT-GFP or GFP

alone. GluA1-CT-GFP expressing CRH neurons did not show augmentation of mEPSC amplitudes after the application of Exn4 (Figure 2M–O). Additionally, in animals with PVN overexpression of GluA1-CT-GFP, the PVN targeted Exn4 injection-induced food intake suppression effects were blunted (Figure 2, P&Q). Interestingly, the expression of GluA1-CT-GFP in PVN itself did not alter basal food intake (Figures S4A&B).

Taken together, these comprehensive data strongly suggest that GLP-1 signaling in the PVN augments CRH neuronal excitatory synaptic strength that likely results from enhanced AMPAR membrane trafficking.

Enhanced trafficking of AMPAR mediates GLP-1R signaling

If our interpretation that GLP-1R signaling facilitates AMPAR trafficking is correct, we should be able to directly examine how changes in signaling cascades downstream of GLP-1R activation affect GluA1 trafficking to the plasma membrane. To address this, we transfected GluA1 and GLP-1R into the mouse brain neuroblastoma cell line Neuro-2a (N2a). After a 15 min treatment with Exn4, a surface biotinylation-labeling assay was employed to isolate membrane proteins (Man et al., 2007), and showed that the membrane expression of GluA1 was dramatically increased by treatment with Exn4 (Figure 3A). Previous reports suggest that GluA1 membrane trafficking is regulated by protein phosphorylation at two sites on the intracellular carboxy terminal motif of the receptor (Roche et al., 1996), i.e. serine 831 (S831), which is phosphorylated by CaMKII and protein kinase C, and serine 845 (S845) which is phosphorylated by PKA (Barria et al., 1997; Mammen et al., 1997; Roche et al., 1996). We asked whether phosphorylation of GluA1 mediates the actions of GLP-1, with the rationale being that GLP-1R activation should increase intracellular cAMP (Drucker et al., 1987) and PKA activation. Unfortunately, the phosphorylation of GluA1 was too low to detect either *in vivo* or *in vitro* in hypothalamic neurons (data not shown). We again used the N2a cell line and enriched GluA1 by first immunoprecipiting (IP) GluA1 utilizing a pH-sensitive form of GFP (Super Ecliptic pHluorin, SEP) tagging, and performed western blotting using phosphorylation site-specific antibodies. Remarkably, we found that phosphorylation of S845, but not S831, was drastically increased after Exn4 treatment (Figure 3B). On the other hand, the phospho-deficient S845A GluA1 mutant failed to respond to GLP-1R activation (Figure 3, A&B). These data strongly suggest that GluA1 S845 is likely a specific target of GLP-1R signaling in the brain.

To further address this hypothesis, we took advantage of a GluA1 S845A knock-in mouse line (Lee et al., 2003) and tested the effects of GLP-1R signaling on synaptic transmission. Remarkably, Exn4 induced up-regulation of mEPSC amplitude on CRH neurons was no longer detected in GluA1 S845A mutant mice (Figure 3C&D). Although S845A mutant mice show normal daily food intake (Figure 3E), the PVN administration of Exn4 induced suppression of food intake was completely blunted (Figure 3F), suggesting S845 phosphorylation of GluA1 is crucial in mediating the effects of GLP-1R on CRH neuronal activation.

To explore the hypothesis that PKA signaling mediates the actions of GLP-1 on AMPAR phosphorylation, we observed that the application of H-89, a PKA blocker, blocked Exn4-

induced GluA1 S845 phosphorylation and surface GluA1 accumulation (Figure 3G&H). However, in addition to the effects on PKA, it is also possible that activation of GLP-1R affects the activity of exchange proteins activated by cAMP (EPAC) (Mangmool et al., 2015) to facilitate GluA1 trafficking. Contrary to this hypothesis, unlike the effects of H-89, application of ESI-09, an EPAC inhibitor, did not block either Exn4 induced membrane GluA1 trafficking or GluA1 phosphorylation (Figure S4, C&D). Thus, we propose that GLP-1 mediated GluA1 membrane trafficking is PKA but not EPAC dependent. Finally, to address the functional significance of our findings that a GLP-1–PKA pathway is likely mediating AMPAR trafficking, we tested whether a blockade of the PKA pathway in the PVN would blunt suppression of food intake elicited by GLP-1R activation. We found that administration of H-89 directly to the PVN was sufficient to block the suppressive effects of Exn4 in the PVN on food intake (Figure 3I&J) while H-89 itself didn't affect food intake (Figure S4, E&F), which may be due to H-89 blockade of Exn4 induced augmentation of mEPSC amplitude in PVN CRH neurons (Figure 3K&L).

Collectively, these data provide strong evidence that GLP-1 mediates synaptic plasticity by specifically increasing the S845 site phosphorylation of GluA1 via the PKA pathway, promoting GluA1 membrane trafficking and augmenting excitatory neurotransmission in the PVN to suppress food intake.

Impaired GLP-1R signaling in the PVN causes obesity

As described previously, week-long stimulation of NTS GCG neurons by hM_3Dq did not affect body weight change in lean mice. Rather, it did significantly decrease the body weight of the obese mice which were fed by high fat food for 5 months (Gaykema et al., 2017). Chemogenetic inhibition of NTS GCG neurons for one week showed a slight increase in the daily food intake but with no obvious body weight gain when compared to control group (Figure S4, L–N). Given the profound effects of GLP-1 signaling in the PVN on food intake (Figure 1, N&O), we asked whether blockade of GLP-1R signaling in the PVN affects energy metabolism and body weight gain. However, a recent study showed that conditional knock out of GLP-1R in Sim-1 neurons in mice had no impact on food intake and body weight (Ghosal et al., 2017). We suspected that, in this instance, a developmental compensatory effect could account for the lack of a feeding phenotype, as *Sim-1* driven Cre expression likely occurs during embryogenesis (Fan et al., 1996). Therefore, we injected AAV-Cre in the PVN of juvenile $GLP\text{-}1R^{f/f}$ animal at 5–6 weeks of age, which resulted in a significant decrease of GLP1-R expression in PVN, but not in the dorsal medial hypothalamus (DMH) or the arcuate nucleus (ARC) (Figure S4 G–J). Remarkably, in the AAV-Cre injected animals, i.e. PVN neuronal GLP-1R knockout mice, we observed a significant gain in body weight when compared to controls (injected with AAV-ΔCre, expressing an inactive Cre-recombinase) in $GLP\text{-}1R^{f/f}$ mice but not in WT animals (Figure 4A&B, Figure S4K). The Cre-injected mice also exhibited an elevation in daily food intake (Figure 4C). With respect to metabolic rate, no difference between O_2 consumption (Figure 4D), CO_2 elimination (Figure 4E) or respiration exchange ratio (Figure 4F) was observed, suggesting that energy expenditure and the selection of fuel substrates were not altered after depletion of GLP-1R in the PVN (Figure 4I). While movement in the X-axis was unaffected, a significant decrease of Z-axis activity when compared to control animals (Figure 4G&H)

was observed. Interestingly, GLP-1R depletion also produced an increase in fasting glucose levels and impaired insulin sensitivity (Figure 4J&K), indicative of insulin resistance. These data suggest that PVN GLP-1R signaling is necessary to maintain energy homeostasis in adult mice.

DISCUSSION

In this study, we unraveled the cellular mechanism underlying a specific neuronal circuit, involving NTS GCG neuronal projections to PVN neurons, which are involved in regulating feeding behavior. Stimulation of the NTS–to–PVN GCG neuronal projection is sufficient to mediate a change in food intake, and GLP-1R expression in the PVN is necessary for regulating food intake as well as maintaining normal body weight. GLP-1 in the PVN likely functions via the following pathway: *1)* GLP-1R signaling activates the PKA signaling pathway which causes *2)* phosphorylation of GluA1 S845 leading to *3)* enhancement of GluA1 membrane trafficking, and finally *4)* augmentation of postsynaptic excitatory synaptic transmission (Fig. 5). This molecular and neuroanatomical pathway identification provides important insight into understanding the functions of endogenous GLP-1 signaling in the PVN and how this circuit could be an effective target for therapies designed to treat obesity.

NTS–to–PVN projecting GLP-1 neurons suppress food intake via activation of GLP-1Rs

It was shown that infusion of Exn4 within the PVN suppresses food intake while Exn9 increases it (Katsurada et al., 2014; McMahon and Wellman, 1998), which suggests GLP-1R signaling in the PVN is sufficient to regulate food intake. In contrast, however, specific ablation of GLP-1R from Sim-1 neurons in PVN doesn't affect food intake and body weight gain, which suggests GLP-1R signaling is not necessary to control feeding behavior (Ghosal et al., 2017). To address this disparity in the data, we used optogenetics to manipulate the activity of the GCG neuron in the presence or absence of glutamate co-release using genetic tools and found that secretion of the GLP-1 peptide independent of glutamate release is sufficient to regulate food intake. Interestingly, the food intake suppression induced by one hour activation of the GCG nerve terminals was shown to last at least one more hour after the completion of photostimulation, which might be due to a delayed recovery in synaptic strength modifications after GLP-1R activation or a prolonged circuit activation downstream of the PVN neuron. Moreover, we also addressed the necessity of the GLP-1R signaling by using loss-function experiments, i.e. optogenetic inhibition as well as PVN GLP-1R KO with both manipulations causing overeating behaviors in animals.

Specific neuronal subtypes within the PVN are thought to drive PVN-dependent anorexia (Darambazar et al., 2015; Otgon-Uul et al., 2016; Santoso et al., 2015; Sedbazar et al., 2014). We identified a large proportion of CRH-expressing PVN neurons that were activated (indicated by the expression of the activity marker c-Fos) following NTS GCG neuronal stimulation. We further substantiated the hypothesis that PVN CRH neurons are a major target of GLP-1 signaling with the following evidence: *1)* over one third of CRH neurons can bind F-Exn4 in vitro, suggesting the presence of GLP-1R expression in those neurons; *2)* CRACM experiments show that over 50% of CRH neurons receive direct projections

from the NTS GCG neurons; *3)* retrograde tracing shows the direct synaptic connection between NTS GCG and PVN CRH neurons; *4)* stimulation of PVN CRH neurons induced an anorexic effect and finally, *5)* inhibition of CRH neuronal activity blocked GLP-1 induced satiety in the PVN. Thus, we suggest CRH neuron activation might contribute to the regulation of food intake behavior induced by endogenous GLP-1. Although CRH is the central player in the hypothalamic-pituitary-adrenal (HPA) axis, previous data shows that stimulation of central GCG neuronal activity by hM_3Dq doesn't affect plasma corticosterone levels, as well as anxiety related behavior (Gaykema et al., 2017). Therefore, CRH mediated GLP-1 satiety effect may not be due to the secondary effect of HPA axis activation.

In addition to CRH neurons in the PVN, other neuronal subtypes, i.e. Sim-1 expressing neurons may also mediate the GLP-1 effect since inhibiting Sim-1 neuronal activity causes a massive increase in feeding (Garfield et al., 2015). Moreover, MC4R expressing neurons, a subset of Sim-1 neurons, also play a pivotal role in food intake (Atasoy et al., 2012). However, inhibition of MC4R neurons alone appeared to cause less increase in food intake when compared to the inhibition of Sim-1 neurons (Atasoy et al., 2012; Garfield et al., 2015), which suggests other subsets of PVN MC4R-negative Sim-1 neurons contribute to food intake regulation. Thus, further work will be required to determine the regulatory functions of GLP-1 in the brain and how this peptide can synergize with these and other modulatory systems.

GLP-1R signaling regulates CRH activity by recruitment of membrane AMPARs

GLP-1 has profound effects on synaptic transmission (for review see: Liu and Pang, 2016), however, the intracellular signaling cascades and pre- or postsynaptic site of action appear to be dependent on brain region and cell type (Acuna-Goycolea and van den Pol, 2004; Korol et al., 2015; Wang et al., 2015). In the current study, we showed that GLP-1R activation by Exn4 facilitates excitatory input in the PVN CRH neurons, in line with the anorexigenic role of this cell type (Hotta et al., 1991; Katsurada et al., 2014). We further provided compelling evidence that a postsynaptic mechanism is involved, most likely via the facilitation of AMPAR trafficking. Initially, we showed that quantal size of EPSCs and the ratio of EPSCs mediated by AMPAR-/NMDAR- in PVN CRH neurons were both increased; Subsequently, we determined that the rectification index of EPSCs, a measure of detecting newly formed AMPAR lacking GluA2, was increased. In addition, IEM1460, a specific GluA2 lacking AMPAR blocker (Gittis et al., 2011; Schlesinger et al., 2005), blunted the effects of Exn4 at synapses, and that the blockade of AMPAR trafficking in the PVN blunted both the food intake suppression effects as well as the facilitation of EPSCs mediated by GLP-1R activation. We conclude that GLP-1R activation induces GluA1 trafficking that facilitates excitatory synaptic drive and increases the excitability of CRH neurons, which may contribute to the suppression of food intake. Although GCG neurons that terminate in the PVN co-release glutamate, glutamate release is not necessary or sufficient for controlling feeding behavior in this neural pathway. The inputs and outputs of the CRH neurons have not been completely characterized and further studies will be needed to determine which afferents mediate the observed modulatory effects of GLP-1 on excitatory glutamatergic transmission in the PVN. Nevertheless a recent paper suggests a small population of glutamatergic neurons in arcuate nucleus of the hypothalamus (ARC) which project to PVN

MC_4R neurons rapidly affect the suppression of food intake (Fenselau et al., 2017). Moreover, this pathway is facilitated by α-MSH postsynaptically. Considering the MC_4R intracellular signaling pathway is the same as that initiated by GLP-1R activation (cAMP-PKA), it is possible that GLP-1 strengthens the excitatory input from ARC glutamate neurons and regulates food intake in a manner similar to that of α-MSH. Our retrograde tracing experiment suggests that PVN CRH neurons receive inputs from DMH, SCN, central amygdala as well as hippocampus (data not shown), areas which could also possibly provide the source of the excitatory input.

With respect to AMPAR trafficking, S831 and S845 phosphorylation in the GluA1 C-terminus has been suggested to be crucial for the recruitment of receptor subunits to the membrane (Barria et al., 1997; Mammen et al., 1997; Roche et al., 1996). While S831 is phosphorylated by PKC and CaMKII, the phosphorylation of which potentiates the single-channel conductance of GluA1-containing AMPARs (Derkach et al., 1999; Derkach, 2003), S845 is phosphorylated by PKA, which increases the open probability (Banke et al., 2000) and surface expression of the receptors (Ehlers, 2000). In the present study, we identified that phosphorylation of S845, but not S831 occurs in response to GLP-1R activation, indicating an involvement of the PKA pathway. Specifically, blocking the PKA pathway inhibits S845 phosphorylation induced by GLP-1 signaling, while the S845A mutation blocked Exn4 induced GluA1 membrane insertion *in vitro*. Collectively, these data suggest that S845 of GluA1 is an important target for GLP-1 signaling. To further support this conclusion, we tested the effects of GLP-1 signaling in a GluA1 S845A knock-in animal model. Strikingly, Exn4 induced suppression of food intake within the PVN was completely blunted in mutant mice and the augmentation of EPSCs mediated by GLP-1R signaling was abolished. These data strongly support our hypothesis that GLP-1R signaling regulates CRH neuron activity by recruitment of membrane AMPARs, likely via PKA phosphorylation of S845 in GluA1.

Loss of function of GLP-1R induces obesity

In addition to investigating the molecular underpinnings of GLP-1R signaling in the PVN, we also tested the physiological relevance of GLP-1R in regulating body weight and metabolic homeostasis. While deletion of GLP-1R in the PVN increased food intake, no effect on metabolic rate was observed. Moreover, the long-term depletion of GLP-1R signaling within the PVN caused a 30% increase in body weight over a six-week period, with mice developing elevated fasted glucose levels and impaired insulin sensitivity. Our work reveals a striking contrast between the mechanism of action of endogenous GLP-1 and that of the systemically administered GLP-1R agonist liraglutide in mediating changes in body weight. While peripheral agonist administration does not require the PVN GLP-1R expression to produce body weight changes (Secher et al., 2014), we show that endogenous GLP-1 signaling does. This discrepancy may be due to the fact that significantly more peripherally administered liraglutide appears to target the arcuate nucleus (ARC) rather than the PVN (Secher et al., 2014), whereas innervation of both structures by GCG neurons is similar in mice (Gaykema et al., 2017; Llewellyn-Smith et al., 2011). Although differences between mouse and rat physiology may also explain the data, prior work in the rat has also failed to show an effect of GLP-1 injection in the ARC on feeding behavior (Sandoval et al.,

2008). Future work will therefore be required to determine whether and to what degree ARC GLP-1R signaling in the mouse mediates an effect of endogenous GLP-1 on body weight homeostasis.

Previous pharmacological studies (i.e. infusion of agonist) suggested that the hypothalamic GLP-1 signal may play a role in the maintenance of glucose homeostasis (Sandoval et al., 2008), however, the ablation of GLP-1R in PVN does not affect glucose metabolism (Burmeister et al., 2017). And a recent report shows that chemogenetic stimulation of endogenous GLP-1 does not affect performance in the glucose and insulin tolerance tests either (Gaykema et al., 2017). Thus, the impaired glucose tolerance and insulin sensitivity we observed in our PVN GLP-1R KO adult mouse model is likely due to the secondary effect of obesity.

While our postnatal viral mediated deletion of GLP-1R from the PVN perturbed body weight homeostasis, the CRH- or Oxt-neuronal specific GLP-1R KO, surprisingly, did not (data not shown). This may have occurred for several reasons: *1)* compensatory pathways may have developed to rescue impaired signaling of GLP-1R within the PVN during development, as GLP-1R was deleted during an early developmental stage, an effect that was likely similar to prior work that showed how *Sim1-Cre* mediated GLP-1R knockout mice had normal food intake and body weight gain (Ghosal et al., 2017); *2)* GLP-1R was not deleted from both CRH and Oxt neurons simultaneously, which may have been required to observe the body weight phenotype, and *3)* GLP-1R signaling in CRH neurons of other brain regions (such as in the central amygdala or brain stem) may exert an opposite role in the regulation of body weight homeostasis when compared to those in the PVN. Nevertheless, based on the viral mediated reduction of GLP-1R expression in the PVN leading to obesity and defects in glucose tolerance, we conclude that GLP-1R is necessary in mediating NTS-to-PVN signaling in central control of metabolic homeostasis.

In summary, this study unravels a previously unidentified molecular cascade, describing the mechanism by which NTS-derived GLP-1 modulates neuronal activity and food intake behavior, while also showing that defective PVN GLP-1 signaling causes obesity (Figure 5). This work provides a framework for studying the mechanism of action of other GPCR coupled receptors in the brain.

STAR methods

Contact for Reagent and Resource Sharing

Further information and requests for resources and reagents should be directed to and will be fulfilled by the Lead Contact, Zhiping Pang (pangzh@rwjms.rutgers.edu) or Michael M. Scott (Michael.scott@virginia.edu).

Experimental Model and Subject Details

Mice—All procedures involving mice were approved by the Rutgers Robert Wood Johnson Medical School Institutional Animal Care and Use Committee (IACUC). All the animals used in this study were 6–8 week old males unless otherwise stated. The animals are bred in the facility at ~22°C and 35–55% humidity. The *Gcg-Cr*e transgene was created by insertion

of Cre-recombinase into the *Gcg* gene locus of BAC RP23-242F22 at the ATG start codon. The BAC transgene was then injected into pronuclei from C57Bl/6j animals to create *Gcg-Cre* transgenic animals (Gaykema et al., 2017). The *CRH-Ires-Cre* (Taniguchi et al., 2011) and *oxytocin (Oxt)-Ires-Cre* mice (Wu et al., 2012) were purchased from Jackson Laboratories (Stock#: 012704 and 024234, respectively). *GLP-1R*$^{f/f}$ mice were described previously (Sisley et al., 2014). The *Vglut2*$^{f/f}$ mice (Tong et al., 2007) were purchased from Jackson Laboratories (Stock#:012898). GluA1 S845A mutant mice were generously provided by Dr. Richard Huganir at the Johns Hopkins University (Lee et al., 2003). Wild type mice C57BL/6 were purchased from Jackson Laboratories. In all cases, mice were randomized according to body weight to each experimental group. The investigator was blinded to the treatment groups except Fig. 1O&Q, Fig. 2Q, Fig. 3F&J, Fig.S1, G. The sample size required was estimated to be n = 7–10 per group on the basis of previous studies examining the effects of GLP-1 on feeding behavior (Wang et al., 2015).

Cell Culture—Neuroblastoma cell line, Neuro-2a (N2a) cells (provided by Dr. Huaye Zhang as a gift, Rutgers University, original source from ATCC and was authenticated by ATCC), were cultured in 10 cm diameter dishes using regular DMEM medium containing 10% heat inactivated fetal bovine serum (FBS, Atlanta Biologics). Cells are kept in incubator: 37°C, 4–10% CO2. Cells are expected in 70–90% confluent for transfection, 6μg GLP-1R (addgene) and 6μg GluA1 (addgene) plasmid are transfected by Lipofectamine 3000 (Life technologies). Cells are harvest 48 hours post-transfection.

Method Details

Virus infection

AAV virus: The AAV-viruses used in this study include: AAV-hSyn-DIO-hM$_3$Dq-mCherry, AAV-hSyn-DIO-hM$_4$Dq-mCherry, AAV-hSyn-DIO-mCherry, AAV-CAG-DIO-tdtomato, AAV-EF1a-DIO-ChR2-YFP, AAV-EF1a-DIO-eArch3.0-YFP or AAV-EF1a-DIO-GFP (purchased from the University of North Carolina Gene Therapy Center); AAV-Cre-GFP and AAV-ΔCre-GFP were generated in house or obtained from Dr. Wei Xu at UT Southwestern Medical Center. The ChR2-YFP encodes a membrane-bound fusion protein, allowing visualization of both the cell bodies and axons of Cre-expressing neurons for morphologic analyses. Viral-mediated protein expression was allowed for a period of 14 days prior to experimental manipulation. Injection sites were confirmed by cutting brain sections and inspecting them under a stereoscope or microscope in all animals reported in this study. 0.6–1μl virus was used for the injection of the Cre-dependent expression AAV virus. For the non-Cre dependent AAV virus, 0.2–0.4μl of virus was injected. The injection speed was 0.1 μl/10min while the injection coordinates for NTS were:

AP: −3.4 mm from lambda; lateral (L): ±0.5 mm; ventral (V): 4.125 mm

The injection coordinates for the PVN were:

AP: −0.94 mm from bregma; lateral (L): ±0.25 mm; ventral (V): 4.75 mm

AAV-Cre injection in GLP-1R$^{f/f}$ mice (PVN)

Each cage of GLP-1R$^{f/f}$ mice (four animals) were divided into two groups: two of them were injected with AAV-Cre virus into the PVN bilaterally using coordinates AP: −0.94; L: ±0.25; V: 4.75. Another two received an injection of control virus (AAV-ΔCre virus).

Retrograde tracing virus: To study the specific projection from GLP-1 positive neurons to PVN CRH neurons, we used a modified rabies virus SADΔG –EGFP (EnvA-SADΔG-EGFP) in combination with Cre-dependent helper AAVs expressing TVA (receptor for the avian sarcoma leucosis virus glycoprotein EnvA; AAV-DIO-tdTomato-TVA) and RG (rabies envelope glycoprotein; AAV-DIO-RV-G). *Gcg:CRH-Cre* double transgenic animals were used in this experiment. AAV-DIO-tdTomato-TVA and AAV-DIO-RV-G (each 0.2μl) were injected into the PVN (AP: −0.94, L: ±0.25; V: 4.75), allowing rabies infection of CRH neurons and subsequent retrograde trans-synaptic spread. Three weeks post-AAV transduction, we injected SADΔG –EGFP into the same area to infect CRH neurons. One week prior to SADΔG –EGFP injection, the Cre-dependent mCherry (AAV-DIO-mCherry) virus was injected into the NTS to label GLP-1 expressing neurons.

Expression of GluR-C termini (CT) by Sindbis virus: Sindbis virus was transfected into PVN neurons, expressing the GFP-tagged cytoplasmic termini of GluA1. GluA1-CT-GFP selectively blocks the trafficking of endogenous GluA1-containing AMPARs as described before (Kielland et al., 2009). The coordinates used for Sindbis virus injection (0.2 μl) in the PVN were: AP −0.94; L: ±0.25; V: 4.75. The *in vivo* behavior testing and *in vitro* recording were performed three days after injection.

PVN cannula placement—The bilateral guide cannulas (Plastics one, C2002DCS-5) or optic fibers (ThorLabs, 200 μm diameter core) (Sparta et al., 2011) were implanted into the PVN and fixed to the skull with cement and three screws. The coordinates used for the PVN were: AP: −0.94; L: ±0.25; V: 4.6 and AP: −0.94; L: ±0.25; V: 4.5 for the guide cannulas and optic fibers, respectively. After surgery, mice were housed individually and were allowed to recover for two weeks before experimentation. The cannula/optic fiber location was checked after sacrifice of animals; data was collected only from animals with proper placement.

Channelrhodopsin (ChR2)-assisted circuit mapping—*Gcg:CRH-Cre* animals were injected by AAV-hSyn-DIO-ChR2-YFP and AAV-hSyn-DIO-tdTomato into NTS and PVN, respectively. Two weeks post-surgery, mice were deeply anesthetized with Euthasol. Coronal hypothalamic slices (300μm) were prepared and whole cell patch clamp recordings were performed at 30°C in ACSF containing (in mM): 125 NaCl, 2.5 KCl, 1.25 NaH_2PO_4, 25 $NaHCO_3$, 2.5 Glucose, 22.5 Sucrose, 2.5 $CaCl_2$, 1.2 $MgCl_2$. Photostimulation-evoked EPSCs were recorded in the whole cell voltage clamp mode, with membrane potential clamped at −70mV. Photostimulation evoked EPSCs were recorded in the presence of picrotoxin (100 μM) to block inhibitory postsynaptic currents. 20 μM CNQX was used to confirm that the response was indeed from EPSCs. All recordings were made using a multiclamp 700B amplifier, and data were filtered at 2 kHz and digitized at 10 kHz. To photostimulate ChR2-positive fibers, a LED light source was used to generate 470nm blue light, which was focused on to the back aperture of the microscope objective, producing a

wide-field exposure of the PVN area. The photostimulation-evoked EPSC detection protocol was described before (Krashes et al., 2014) and involved four blue light laser pulses administered 1 s apart during the first 4 s of an 8 s sweep, repeated for a total of 16 sweeps.

Immunohistochemistry (IHC)—Mice were deeply anesthetized with Euthasol and transcardially perfused with 4% PFA in PBS, pH 7.4. Coronal brain slices (45 μm) were prepared and a standard IHC protocol was followed. The primary antibodies used were anti-c-Fos (1:1000, Santa Cruz, SC-271243); anti-AVP (1:1000, Millipore, ab 1565); anti-OXT (1:1000, Millipore, ab 911). AlexaFluor secondary antibodies (633-goat anti-mouse, 1:1000; 546-goat anti-rabbit, 1:1000, Life Technologies, A21052 and A11035 respectively) were used to visualize the signal and images were acquired by confocal microscopy (Zeiss, LSM700).

Live cell labeling with F-Exn4—The *CRH-Ires-Cre* mice were injected with AAV-DIO-mCherry. Two weeks after, mice were sacrificed and coronal hypothalamic slices (300 μm) were incubated at 30°C for 20 min in oxygenated artificial cerebrospinal fluid (ACSF) containing (in mM): 125 NaCl, 2.5 KCl,1.25 NaH_2PO_4, 25 $NaHCO_3$, 2.5 Glucose, 22.5 Sucrose, 2.5 $CaCl_2$, 1.2 $MgCl_2$. The slices were incubated with 100 nM Fluorescein-Trp^{25}-Exendin-4 (F-Exn4, Anaspec Inc., cat # AS-63899) in ACSF at room temperature for 15 min. 4% PFA was used to fix the tissue directly after removing ACSF. The slices were washed well with PBS prior to immunostaining. The primary antibodies used were: anti-OXT (1:1000, Millipore, ab911); anti-AVP (1:1000, Millipore, ab1565). The secondary antibodies used were: Alex-546-goat anti-rabbit (1:1000, Life Technologies, A11035) and Alex-633-goat anti-mouse (1:1000, Life Technologies, A21052).

Behavior experiments

Optogenetic manipulation of GLP-1 fibers: Optical fibers (200 μm diameter core), NA 0.37 (Thorlabs) were coupled to a fiber optic rotary joint (Prizmatix) and the LED generator (470nm for stimulation, Prizmatix UHP-T-470-LA, 530nm for inhibition, Thorlabs M530F2). A terminal fiber attached to the rotary joint was coupled to a 1.25 OD zirconium ferrule and a mating sleeve which allowed delivery of light to the brain. For in vivo photo-stimulation experiments, 5 ms pulses 470nm blue light were given as 10 pulses/s every 4s for one hour. For the in vivo photo-inhibition experiments, 10min constant 530nm green light intervals with 5min breaks between stimulation were administered for 1hr. For the stimulation experiment, animals were provided only 0.5g food overnight. For the inhibition experiment, animals were provided 1.2–1.5g food overnight. All the mice were trained for 4 days to acclimate to the feeding schedule. Food intake was measured at 0.5hr, 1hr, 2hrs and 5hrs.

Excitatory/inhibitory DREADDs: For local stimulation of GLP-1 fibers in the PVN, *Gcg-Cre* mice were injected with hM_3Dq AAV virus in the NTS. After 2 weeks recovery, 5μM (200nl) of CNO (Tocris) was used for intracranial injection into the PVN through a guide cannula. Food intake was monitored 30min post-injection. To block GLP-1 receptor activation in the PVN, Exendin 9–39 (Exn9) was injected into the PVN through the guide cannula 10 min prior to CNO injection. For inhibition of NTS GLP-1 neurons, hM_4Di AAV

virus was injected 2 weeks prior to CNO injection. 0.3mg/kg CNO was given by i.p. injection every day at 6:00pm for one week. Food intake and body weight were monitored every day.

To stimulate endogenous CRH neurons, *CRH-Cre* mice were injected with hM_3Dq AAV virus in PVN. After 2 weeks recovery, 0.3mg/kg CNO was given by i.p. injection. Food intake was monitored 30min later.

Exciting GLP-1 and inhibiting CRH: We injected AAV-DIO-ChR2 and AAV-DIO-hM_4Di into NTS and PVN, respectively, in *Gcg:CRH-Cre* transgenic animals. After 2 weeks recovery, the mice were trained for an additional four days to consume 0.5g of food overnight and received an i.p. injection of phosphate-buffered saline (PBS, 100μl). From the 5^{th} to 8^{th} day, the animals were treated with: PBS only, CNO only (0.3mg/kg), PBS (30min prior) + blue light, CNO (30min prior) + blue light respectively. Food intake was monitored at t=30min,1hr and 2hrs from the fifth day.

PKA-GluA1 pathway effect on food intake: To study the GluA1 mediated GLP-1 anorexigenic effect, we randomly divided the mice into three groups: control + vehicle (Veh, sindbis virus-GFP + intra-PVN injection of saline); control + Exn4 (sindbis virus-GFP + intra-PVN injection of 0.1μg/200nl Exn4); and GluA1-CT + Exn4 (sindbis virus-GluA1-CT-GFP + intra-PVN injection of 0.1μg/200nl Exn4). Food was measured at t=0, 30, 60, and 120 min after injection.

To study how the phosphorylation of GluA1 effected food intake, we injected either vehicle (200nl saline) or Exn4 (0. 1μg/200nl) into the PVN of control (WT mice) and mutant (GluA1 S845 Knock-in) mice using a guide cannula.

To block the PKA pathway in the PVN, 500nl (5μM) of the PKA inhibitor H-89 was locally injected through the guide cannula 10min prior to delivery of Exn4 into PVN of WT animals.

Depletion of GLP-1R in PVN: Body weight was monitored every week post-surgery (week 0). On week three, animals were separated into individual cages to adapt to their surroundings for one day. Food intake was measured on the third day. During week 6, all the animals were placed into metabolic cages (Columbus Instruments, Comprehensive Lab Animal Monitoring System (CLAMS), OH, USA) to adapt to their surroundings 12 hours before measurement. All metabolic data was collected in night phase. For the insulin tolerance test during week 6, animals were fasted overnight. The baseline plasma glucose was measured by glucometer (FreeStyle Lite system, Abbott Diabetes Care Inc. CA, USA) at t=0. Then 0.75U/kg insulin was systemically injected immediately after baseline samples. The plasma glucose was measured at t=15, 30, 60, and 120 min after insulin injection.

Electrophysiology

Electrophysiology was performed as described previously (Pang et al., 2002) with minor modifications. Briefly, mice were deeply anesthetized with Euthasol. Coronal hypothalamic slices (300 μm) were prepared and whole cell patch clamp recordings were performed at

30°C in ACSF containing (in mM): 125 NaCl, 2.5 KCl, 1.25 NaH_2PO_4, 25 $NaHCO_3$, 2.5 Glucose, 22.5 Sucrose, 2.5 $CaCl_2$, 1.2 $MgCl_2$. Patch pipettes (3.5–6 MΩ) were pulled from borosilicate glass and filled with internal solution containing (in mM): 40 CsCl, 90 K-Gluconate, 10 HEPES, 0.05 EGTA, 1.8 NaCl, 3.5 KCl, 1.7 $MgCl_2$, 2 Mg-ATP, 0.4 Na_4-GTP, 10 Phosphocreatine and additional 5mM QX-314 for evoked EPSCs. CRH neurons were labeled by a previous injection of AAV-DIO-mCherry into the PVN of *CRH-Ires-Cre* mice. Whole cell patch clamp recordings were performed using an Axon 700B amplifier. Data were filtered at 2 kHz, digitized at 10 kHz and collected using Clampex 10.2 (Molecular Devices). To record EPSCs, picrotoxin (50 μM, Sigma) was added to block IPSCs mediated by $GABA_A$ receptors. TTX (1 μM) was added to block action potentials for mEPSCs recording. To isolate AMPAR-mediated evoked responses, the NMDAR antagonist D-APV (50 μM) was added to the perfusion buffer. A bipolar stimulating electrode was placed 100–300 μm lateral to the recording electrode, and was used to stimulate efferents at 0.05 Hz. Neurons were voltage-clamped at −70 mV to record AMPAR-mediated EPSCs and at +40 mV to record dual-component EPSCs containing NMDAR EPSCs. AMPAR/NMDAR ratios were also calculated by dividing the peak of the AMPAR EPSC at −70 mV by the value of the NMDAR EPSC after stimulation start time 50ms at +40 mV. Evoked IV curve was performed at: −70mV, −40mV, 0, +40mV, and +60mV. PTX and APV were applied to block GABA and NMDA receptor. 100μM spermine was included in the internal solution. 50μM IEM-1460 was used to block GluA1 lacking Ca^{2+} permeable AMPA receptor. Furthermore, since Exn4 (10nM) was reported to be sufficient for enhancement of both the synaptic and tonic GABA-activated currents (Korol et al., 2015), we selected this concentration for bath application of Exn4 to stimulate GLP-1R within the PVN. H-89 (10μM) was applied to block the PKA pathway.

In vitro biochemistry studies

Neuroblastoma cell line, Neuro-2a (N2a) cells (provided by Dr. Huaye Zhang as a gift, original source from ATCC, CCL-131, Rutgers University), were cultured in 10 cm diameter dishes using regular DMEM medium supplemented with 10% fetal bovine serum (FBS, Atlanta Biologics).

For the GFP-GluA1 Co-IP experiment, N2a cells were transfected with GLP-1R and GFP-GluA1 plasmids (except negative control, which was only transfected with GLP-1R plasmid). Three days post-transfection, cells were cultured at 37°C for 15min in the presence of either: 1) 0.1% DMSO, control; 2) H-89, 10μM (dissolved in DMSO); 3) Exn4, 10nM Exn4 + 0.1%DMSO; 4) H-89 + Exn4, 10nM Exn4 + 10μM H-89. GluA1 protein was pulled down with GFP-Trap, a high quality GFP binding protein coupled to a monovalent matrix (Chromotek, Planegg-Martinsried, Germany). Immunoblotting was performed with GluA1 Ser831 and Ser845 phosphorylation specific antibodies (Abcam, ab109464 and ab76321, respectively, 1:500 each), anti-GFP (Abcam, ab13970, 1:500), β-actin (Sigma, A5441, 1:5000). HRP-anti-mouse (1:10000, Life Technologies), HRP-anti-rabbit (1:10000, Life Technologies) and HRP-anti-chicken (1:5000, Santa Cruz) were used to detect the signal.

For the biotinylation assays, the N2a cells were transfected with a plasmid encoding GLP-1R and cultured in 10 cm diameter dishes. Three days post-transfection, cells were

treated with: 1) 0.1% DMSO, control; 2) H-89, 10μM H-89 (dissolved in DMSO); 3) Exn4, 10nM Exn4 + 0.1%DMSO; 4) H-89 + Exn4, 10nM Exn4 + 10μM H-89, and incubated in 37°C for 15min. After washing well with PBS, cells were incubated with 10mM Sulfo-NHS-SS-Biotin (Thermo Scientific, 21331) for 30 min before lysis. Immunoprecipitated proteins were then pulled down by incubating with NeutrAvidin Agarose Resins (Thermo Scientific, 29200) at 4°C overnight. The samples were then immunoblotted using an anti-GluA1 antibody (Abcam, ab86141).

For S845A mutation experiments, the same conditions were used as described above. The experimental groups were divided into: 1) WT-GluA1 + control (0.1%DMSO); 2) WT-GluA1 + Exn4 (10nM Exn4 in 0.1%DMSO); 3) Mutant-GluA1 + control (0.1%DMSO); 4) Mutant-GluA1 + Exn4 (10nM Exn4 in 0.1%DMSO). Each study was repeated on three occasions each with four replicates for the biotinylation assay.

Quantification and Statistical Analysis

Statistical analysis was performed using SPSS (version 18) or Excel (version 2013). We first determined if the data values came from a normal distribution by Kolmogorov–Smirnov test. Repeated measurement 2-way ANOVA and post-hoc Bonferroni tests were used for all time-dependent experiments. Fig. 1C&D, Fig. 2L, Fig. 3E, F&J, Fig. 4C–J, Fig.S1, B, I, K&L, Fig.S4, B&F use one-way ANOVA (plus post-hoc t-test if applicable). Fig. 1Q, Fig.S1G and all EPSCs amplitudes and frequency were compared by paired-t-test. The cumulative frequency curve was analyzed by the Kolmogorov-Smirnov test. Statistical significance was set at $p < 0.05$. All the details of experiments can be found in the figure legends. All data values are presented as mean ± SEM.

Supplementary Material

Refer to Web version on PubMed Central for supplementary material.

Acknowledgments

We thank Drs. Arnold Rabson, Weiping Han, Nicholas Bello, Ami Citri, Nicola Francis for critical reading of this manuscript. We thank Dr. Sally Radovick for providing Comprehensive Lab Animal Monitoring System (CLAMS). We thank Dr. Wei Xu of UT Southwestern Medical Center for providing AAV-Cre and Delta-Cre viruses. We thank Dr. Richard Huganir from Johns Hopkins University for providing the GluA1S845A mutant mice. Dr. Seeley serves as consultant or scientific advisory board member, or is receiving research supported from Orexigen; Novo Nordisk, Daiichi Sankyo, Jenssen/Johnson & Johnson, Novartis, Paulk Hastings Law Firm, Zafgen, MedImmune, Sanofi, Kallyope. The research is funded by the American Heart Association postdoctoral fellowship (16POST27710022), the US-Israel Binational Science Foundation (BSF), the Robert Wood Johnson Foundation, and the Sinsheimer Foundation. The Pang laboratory is supported by NIH-NIAAA AA023797.

References

Acuna-Goycolea C, van den Pol A. Glucagon-like peptide 1 excites hypocretin/orexin neurons by direct and indirect mechanisms: implications for viscera-mediated arousal. The Journal of neuroscience : the official journal of the Society for Neuroscience. 2004; 24:8141–8152. [PubMed: 15371515]

Atasoy D, Betley JN, Su HH, Sternson SM. Deconstruction of a neural circuit for hunger. Nature. 2012; 488:172–177. [PubMed: 22801496]

Banke TG, Bowie D, Lee H, Huganir RL, Schousboe A, Traynelis SF. Control of GluR1 AMPA receptor function by cAMP-dependent protein kinase. The Journal of neuroscience : the official journal of the Society for Neuroscience. 2000; 20:89–102. [PubMed: 10627585]

Barria A, Derkach V, Soderling T. Identification of the Ca2+/calmodulin-dependent protein kinase II regulatory phosphorylation site in the alpha-amino-3-hydroxyl-5-methyl-4-isoxazole-propionate-type glutamate receptor. The Journal of biological chemistry. 1997; 272:32727–32730. [PubMed: 9407043]

Betley JN, Cao ZF, Ritola KD, Sternson SM. Parallel, redundant circuit organization for homeostatic control of feeding behavior. Cell. 2013; 155:1337–1350. [PubMed: 24315102]

Burmeister MA, Ayala JE, Smouse H, Landivar-Rocha A, Brown JD, Drucker DJ, Stoffers DA, Sandoval DA, Seeley RJ, Ayala JE. The Hypothalamic Glucagon-Like Peptide 1 Receptor Is Sufficient but Not Necessary for the Regulation of Energy Balance and Glucose Homeostasis in Mice. Diabetes. 2017; 66:372–384. [PubMed: 27908915]

Citri A, Malenka RC. Synaptic plasticity: multiple forms, functions, and mechanisms. Neuropsychopharmacology. 2008; 33:18–41. [PubMed: 17728696]

Cork SC, Richards JE, Holt MK, Gribble FM, Reimann F, Trapp S. Distribution and characterisation of Glucagon-like peptide-1 receptor expressing cells in the mouse brain. Molecular metabolism. 2015; 4:718–731. [PubMed: 26500843]

Darambazar G, Nakata M, Okada T, Wang L, Li E, Shinozaki A, Motoshima M, Mori M, Yada T. Paraventricular NUCB2/nesfatin-1 is directly targeted by leptin and mediates its anorexigenic effect. Biochemical and biophysical research communications. 2015; 456:913–918. [PubMed: 25534851]

Derkach V, Barria A, Soderling TR. Ca2+/calmodulin-kinase II enhances channel conductance of alpha-amino-3-hydroxy-5-methyl-4-isoxazolepropionate type glutamate receptors. Proceedings of the National Academy of Sciences of the United States of America. 1999; 96:3269–3274. [PubMed: 10077673]

Derkach VA. Silence analysis of AMPA receptor mutated at the CaM-kinase II phosphorylation site. Biophysical journal. 2003; 84:1701–1708. [PubMed: 12609872]

Drucker DJ, Philippe J, Mojsov S, Chick WL, Habener JF. Glucagon-like peptide I stimulates insulin gene expression and increases cyclic AMP levels in a rat islet cell line. Proceedings of the National Academy of Sciences of the United States of America. 1987; 84:3434–3438. [PubMed: 3033647]

Ehlers MD. Reinsertion or degradation of AMPA receptors determined by activity-dependent endocytic sorting. Neuron. 2000; 28:511–525. [PubMed: 11144360]

Fan CM, Kuwana E, Bulfone A, Fletcher CF, Copeland NG, Jenkins NA, Crews S, Martinez S, Puelles L, Rubenstein JL, Tessier-Lavigne M. Expression patterns of two murine homologs of Drosophila single-minded suggest possible roles in embryonic patterning and in the pathogenesis of Down syndrome. Mol Cell Neurosci. 1996; 7:1–16. [PubMed: 8812055]

Fenselau H, Campbell JN, Verstegen AM, Madara JC, Xu J, Shah BP, Resch JM, Yang Z, Mandelblat-Cerf Y, Livneh Y, Lowell BB. A rapidly acting glutamatergic ARC-->PVH satiety circuit postsynaptically regulated by alpha-MSH. Nature neuroscience. 2017; 20:42–51. [PubMed: 27869800]

Garfield AS, Li C, Madara JC, Shah BP, Webber E, Steger JS, Campbell JN, Gavrilova O, Lee CE, Olson DP, et al. A neural basis for melanocortin-4 receptor-regulated appetite. Nature neuroscience. 2015; 18:863–871. [PubMed: 25915476]

Gaykema RP, Newmyer BA, Ottolini M, Raje V, Warthen DM, Lambeth PS, Niccum M, Yao T, Huang Y, Schulman IG, et al. Activation of murine pre-proglucagon-producing neurons reduces food intake and body weight. The Journal of clinical investigation. 2017; 127:1031–1045. [PubMed: 28218622]

Ghosal S, Packard AE, Mahbod P, McKlveen JM, Seeley RJ, Myers B, Ulrich-Lai Y, Smith EP, D'Alessio DA, Herman JP. Disruption of Glucagon-Like Peptide 1 Signaling in Sim1 Neurons Reduces Physiological and Behavioral Reactivity to Acute and Chronic Stress. The Journal of neuroscience : the official journal of the Society for Neuroscience. 2017; 37:184–193. [PubMed: 28053040]

Gittis AH, Leventhal DK, Fensterheim BA, Pettibone JR, Berke JD, Kreitzer AC. Selective inhibition of striatal fast-spiking interneurons causes dyskinesias. The Journal of neuroscience : the official journal of the Society for Neuroscience. 2011; 31:15727–15731. [PubMed: 22049415]

Gu G, Roland B, Tomaselli K, Dolman CS, Lowe C, Heilig JS. Glucagon-like peptide-1 in the rat brain: distribution of expression and functional implication. J Comp Neurol. 2013; 521:2235–2261. [PubMed: 23238833]

Hallbrink M, Holmqvist T, Olsson M, Ostenson CG, Efendic S, Langel U. Different domains in the third intracellular loop of the GLP-1 receptor are responsible for Galpha(s) and Galpha(i)/Galpha(o) activation. Biochimica et biophysica acta. 2001; 1546:79–86. [PubMed: 11257510]

Holst JJ. The physiology of glucagon-like peptide 1. Physiological reviews. 2007; 87:1409–1439. [PubMed: 17928588]

Hotta M, Shibasaki T, Yamauchi N, Ohno H, Benoit R, Ling N, Demura H. The effects of chronic central administration of corticotropin-releasing factor on food intake, body weight, and hypothalamic-pituitary-adrenocortical hormones. Life sciences. 1991; 48:1483–1491. [PubMed: 1849215]

Katsurada K, Maejima Y, Nakata M, Kodaira M, Suyama S, Iwasaki Y, Kario K, Yada T. Endogenous GLP-1 acts on paraventricular nucleus to suppress feeding: projection from nucleus tractus solitarius and activation of corticotropin-releasing hormone, nesfatin-1 and oxytocin neurons. Biochemical and biophysical research communications. 2014; 451:276–281. [PubMed: 25089000]

Kielland A, Bochorishvili G, Corson J, Zhang L, Rosin DL, Heggelund P, Zhu JJ. Activity patterns govern synapse-specific AMPA receptor trafficking between deliverable and synaptic pools. Neuron. 2009; 62:84–101. [PubMed: 19376069]

Korol SV, Jin Z, Babateen O, Birnir B. GLP-1 and exendin-4 transiently enhance GABAA receptor-mediated synaptic and tonic currents in rat hippocampal CA3 pyramidal neurons. Diabetes. 2015; 64:79–89. [PubMed: 25114295]

Krashes MJ, Shah BP, Madara JC, Olson DP, Strochlic DE, Garfield AS, Vong L, Pei H, Watabe-Uchida M, Uchida N, et al. An excitatory paraventricular nucleus to AgRP neuron circuit that drives hunger. Nature. 2014; 507:238–242. [PubMed: 24487620]

Larsen PJ, Tang-Christensen M, Holst JJ, Orskov C. Distribution of glucagon-like peptide-1 and other preproglucagon-derived peptides in the rat hypothalamus and brainstem. Neuroscience. 1997; 77:257–270. [PubMed: 9044391]

Lee HK, Takamiya K, Han JS, Man H, Kim CH, Rumbaugh G, Yu S, Ding L, He C, Petralia RS, et al. Phosphorylation of the AMPA receptor GluR1 subunit is required for synaptic plasticity and retention of spatial memory. Cell. 2003; 112:631–643. [PubMed: 12628184]

Liu J, Pang ZP. Glucagon-like peptide-1 drives energy metabolism on the synaptic highway. The FEBS journal. 2016

Llewellyn-Smith IJ, Reimann F, Gribble FM, Trapp S. Preproglucagon neurons project widely to autonomic control areas in the mouse brain. Neuroscience. 2011; 180:111–121. [PubMed: 21329743]

Mammen AL, Kameyama K, Roche KW, Huganir RL. Phosphorylation of the alpha-amino-3-hydroxy-5-methylisoxazole4-propionic acid receptor GluR1 subunit by calcium/calmodulin-dependent kinase II. The Journal of biological chemistry. 1997; 272:32528–32533. [PubMed: 9405465]

Man HY, Sekine-Aizawa Y, Huganir RL. Regulation of {alpha}-amino-3-hydroxy-5-methyl-4-isoxazolepropionic acid receptor trafficking through PKA phosphorylation of the Glu receptor 1 subunit. Proceedings of the National Academy of Sciences of the United States of America. 2007; 104:3579–3584. [PubMed: 17360685]

Mangmool S, Hemplueksa P, Parichatikanond W, Chattipakorn N. Epac is required for GLP-1R-mediated inhibition of oxidative stress and apoptosis in cardiomyocytes. Mol Endocrinol. 2015; 29:583–596. [PubMed: 25719403]

McCormack SG, Stornetta RL, Zhu JJ. Synaptic AMPA receptor exchange maintains bidirectional plasticity. Neuron. 2006; 50:75–88. [PubMed: 16600857]

McMahon LR, Wellman PJ. PVN infusion of GLP-1-(7-36) amide suppresses feeding but does not induce aversion or alter locomotion in rats. The American journal of physiology. 1998; 274:R23–29. [PubMed: 9458894]

Mietlicki-Baase EG, Ortinski PI, Reiner DJ, Sinon CG, McCutcheon JE, Pierce RC, Roitman MF, Hayes MR. Glucagon-like peptide-1 receptor activation in the nucleus accumbens core suppresses feeding by increasing glutamatergic AMPA/kainate signaling. The Journal of neuroscience : the official journal of the Society for Neuroscience. 2014; 34:6985–6992. [PubMed: 24828651]

Mietlicki-Baase EG, Ortinski PI, Rupprecht LE, Olivos DR, Alhadeff AL, Pierce RC, Hayes MR. The food intake-suppressive effects of glucagon-like peptide-1 receptor signaling in the ventral tegmental area are mediated by AMPA/kainate receptors. American journal of physiology Endocrinology and metabolism. 2013; 305:E1367–1374. [PubMed: 24105414]

Montrose-Rafizadeh C, Avdonin P, Garant MJ, Rodgers BD, Kole S, Yang H, Levine MA, Schwindinger W, Bernier M. Pancreatic glucagon-like peptide-1 receptor couples to multiple G proteins and activates mitogen-activated protein kinase pathways in Chinese hamster ovary cells. Endocrinology. 1999; 140:1132–1140. [PubMed: 10067836]

Olson BR, Drutarosky MD, Chow MS, Hruby VJ, Stricker EM, Verbalis JG. Oxytocin and an oxytocin agonist administered centrally decrease food intake in rats. Peptides. 1991; 12:113–118. [PubMed: 1646995]

Otgon-Uul Z, Suyama S, Onodera H, Yada T. Optogenetic activation of leptin- and glucose-regulated GABAergic neurons in dorsomedial hypothalamus promotes food intake via inhibitory synaptic transmission to paraventricular nucleus of hypothalamus. Molecular metabolism. 2016; 5:709–715. [PubMed: 27656408]

Pang ZP, Deng P, Ruan YW, Xu ZC. Depression of fast excitatory synaptic transmission in large aspiny neurons of the neostriatum after transient forebrain ischemia. The Journal of neuroscience : the official journal of the Society for Neuroscience. 2002; 22:10948–10957. [PubMed: 12486190]

Rajan S, Dickson LM, Mathew E, Orr CM, Ellenbroek JH, Philipson LH, Wicksteed B. Chronic hyperglycemia downregulates GLP-1 receptor signaling in pancreatic beta-cells via protein kinase A. Molecular metabolism. 2015; 4:265–276. [PubMed: 25830090]

Reiner DJ, Mietlicki-Baase EG, McGrath LE, Zimmer DJ, Bence KK, Sousa GL, Konanur VR, Krawczyk J, Burk DH, Kanoski SE, et al. Astrocytes Regulate GLP-1 Receptor-Mediated Effects on Energy Balance. The Journal of neuroscience : the official journal of the Society for Neuroscience. 2016; 36:3531–3540. [PubMed: 27013681]

Roche KW, O'Brien RJ, Mammen AL, Bernhardt J, Huganir RL. Characterization of multiple phosphorylation sites on the AMPA receptor GluR1 subunit. Neuron. 1996; 16:1179–1188. [PubMed: 8663994]

Sandoval DA, Bagnol D, Woods SC, D'Alessio DA, Seeley RJ. Arcuate glucagon-like peptide 1 receptors regulate glucose homeostasis but not food intake. Diabetes. 2008; 57:2046–2054. [PubMed: 18487451]

Santoso P, Maejima Y, Kumamoto K, Takenoshita S, Shimomura K. Central action of ELABELA reduces food intake and activates arginine vasopressin and corticotropin-releasing hormone neurons in the hypothalamic paraventricular nucleus. Neuroreport. 2015; 26:820–826. [PubMed: 26237243]

Schlesinger F, Tammena D, Krampfl K, Bufler J. Two mechanisms of action of the adamantane derivative IEM-1460 at human AMPA-type glutamate receptors. British journal of pharmacology. 2005; 145:656–663. [PubMed: 15834439]

Secher A, Jelsing J, Baquero AF, Hecksher-Sorensen J, Cowley MA, Dalboge LS, Hansen G, Grove KL, Pyke C, Raun K, et al. The arcuate nucleus mediates GLP-1 receptor agonist liraglutide-dependent weight loss. The Journal of clinical investigation. 2014; 124:4473–4488. [PubMed: 25202980]

Sedbazar U, Ayush EA, Maejima Y, Yada T. Neuropeptide Y and alpha-melanocyte-stimulating hormone reciprocally regulate nesfatin-1 neurons in the paraventricular nucleus of the hypothalamus. Neuroreport. 2014; 25:1453–1458. [PubMed: 25383463]

Shor-Posner G, Azar AP, Insinga S, Leibowitz SF. Deficits in the control of food intake after hypothalamic paraventricular nucleus lesions. Physiology & behavior. 1985; 35:883–890. [PubMed: 3006098]

Sims JS, Lorden JF. Effect of paraventricular nucleus lesions on body weight, food intake and insulin levels. Behavioural brain research. 1986; 22:265–281. [PubMed: 3098259]

Sisley S, Gutierrez-Aguilar R, Scott M, D'Alessio DA, Sandoval DA, Seeley RJ. Neuronal GLP1R mediates liraglutide's anorectic but not glucose-lowering effect. The Journal of clinical investigation. 2014; 124:2456–2463. [PubMed: 24762441]

Sparta DR, Stamatakis AM, Phillips JL, Hovelso N, van Zessen R, Stuber GD. Construction of implantable optical fibers for long-term optogenetic manipulation of neural circuits. Nature protocols. 2011; 7:12–23. [PubMed: 22157972]

Sutton AK, Pei H, Burnett KH, Myers MG Jr, Rhodes CJ, Olson DP. Control of food intake and energy expenditure by Nos1 neurons of the paraventricular hypothalamus. The Journal of neuroscience : the official journal of the Society for Neuroscience. 2014; 34:15306–15318. [PubMed: 25392498]

Takahashi T, Svoboda K, Malinow R. Experience strengthening transmission by driving AMPA receptors into synapses. Science. 2003; 299:1585–1588. [PubMed: 12624270]

Taniguchi H, He M, Wu P, Kim S, Paik R, Sugino K, Kvitsiani D, Fu Y, Lu J, Lin Y, et al. A resource of Cre driver lines for genetic targeting of GABAergic neurons in cerebral cortex. Neuron. 2011; 71:995–1013. [PubMed: 21943598]

Thorens B. Expression cloning of the pancreatic beta cell receptor for the gluco-incretin hormone glucagon-like peptide 1. Proceedings of the National Academy of Sciences of the United States of America. 1992; 89:8641–8645. [PubMed: 1326760]

Thorens B, Porret A, Buhler L, Deng SP, Morel P, Widmann C. Cloning and functional expression of the human islet GLP-1 receptor. Demonstration that exendin-4 is an agonist and exendin-(9-39) an antagonist of the receptor. Diabetes. 1993; 42:1678–1682. [PubMed: 8405712]

Tong Q, Ye C, McCrimmon RJ, Dhillon H, Choi B, Kramer MD, Yu J, Yang Z, Christiansen LM, Lee CE, et al. Synaptic glutamate release by ventromedial hypothalamic neurons is part of the neurocircuitry that prevents hypoglycemia. Cell metabolism. 2007; 5:383–393. [PubMed: 17488640]

Turton MD, O'Shea D, Gunn I, Beak SA, Edwards CM, Meeran K, Choi SJ, Taylor GM, Heath MM, Lambert PD, et al. A role for glucagon-like peptide-1 in the central regulation of feeding. Nature. 1996; 379:69–72. [PubMed: 8538742]

Wang XF, Liu JJ, Xia J, Liu J, Mirabella V, Pang ZP. Endogenous Glucagon-like Peptide-1 Suppresses High-Fat Food Intake by Reducing Synaptic Drive onto Mesolimbic Dopamine Neurons. Cell reports. 2015; 12:726–733. [PubMed: 26212334]

Wheeler MB, Lu M, Dillon JS, Leng XH, Chen C, Boyd AE 3rd. Functional expression of the rat glucagon-like peptide-I receptor, evidence for coupling to both adenylyl cyclase and phospholipase-C. Endocrinology. 1993; 133:57–62. [PubMed: 8391428]

Wu Z, Xu Y, Zhu Y, Sutton AK, Zhao R, Lowell BB, Olson DP, Tong Q. An obligate role of oxytocin neurons in diet induced energy expenditure. PloS one. 2012; 7:e45167. [PubMed: 23028821]

Zheng H, Stornetta RL, Agassandian K, Rinaman L. Glutamatergic phenotype of glucagon-like peptide 1 neurons in the caudal nucleus of the solitary tract in rats. Brain structure & function. 2015; 220:3011–3022. [PubMed: 25012114]

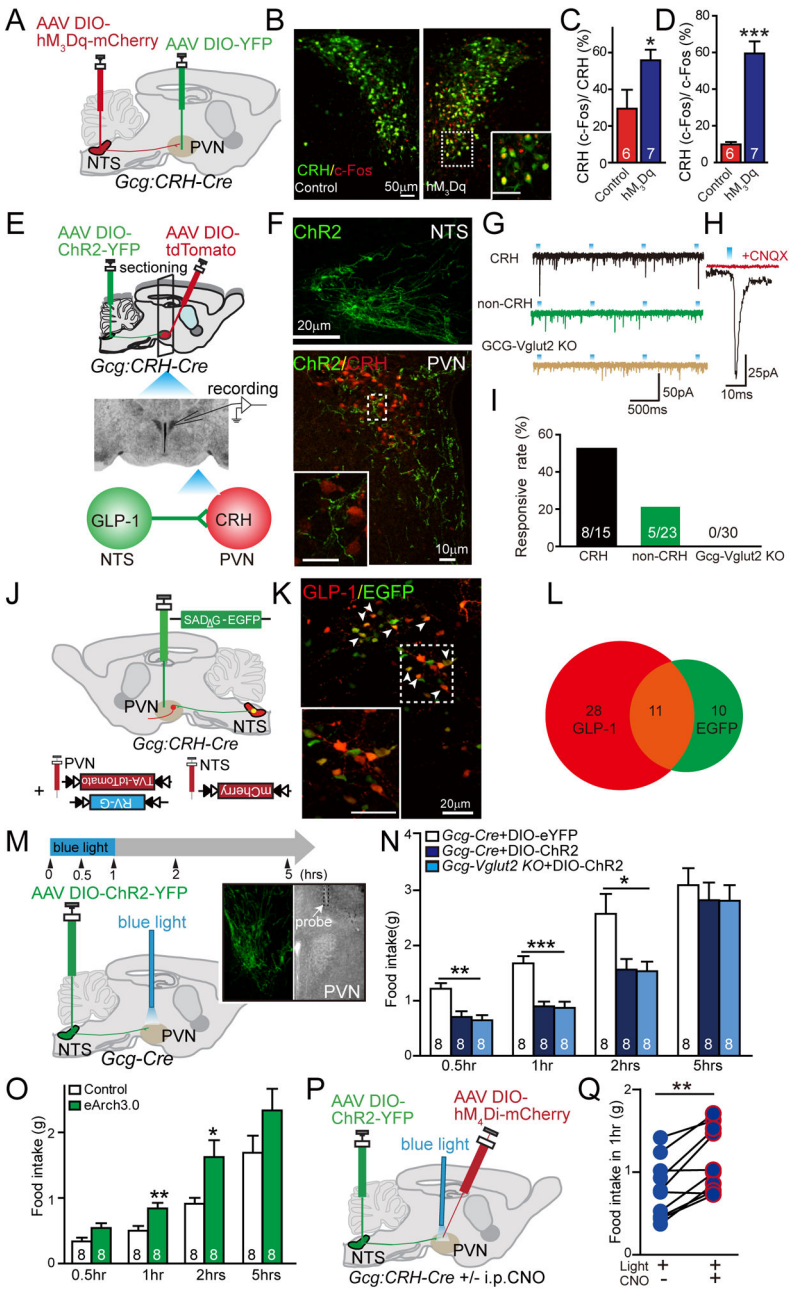

Figure 1. NTS→PVN GLP-1 signaling suppresses food intake

A, Experimental paradigm for chemogenetic stimulation of endogenous GLP-1 neurons. **B,** Increased c-Fos expression in CRH neurons (labeled by Cre-dependent YFP expression) after chemogenetic activation of GCG neurons. **C&D**, Quantification of c-Fos and CRH co-localized neurons. **E**, Experimental paradigm for ChR2-assisted circuit mapping (CRACM). **F**, *Top panel*, Cre-dependent ChR2 expression in NTS; *bottom panel*, GLP-1 afferents and CRH neurons (labeled by Cre-dependent tdTomato) in PVN. *Insert* showing the magnified image of the dash square indicated area. **G**, Representative trace of the photostimulation (470 nm LED) evoked synaptic currents in CRH-, non-CRH-neurons in control mice and

PVN neurons in Gcg-*Vglut2 KO* mice (in 100μM PTX). **H** Single light evoked EPSC, which can be blocked by CNQX. **I**, Percentage of neurons showing synaptic connections (numbers indicate the numbers of responsive cells/total cells). **J,** Experimental paradigm for pseudorabies virus retrograde tracing. **K,** Rabies viral mediated expression of EGFP in NTS GLP-1 neurons. **L,** Quantitation of the retrograde labeled cells. **M**, Experimental paradigm for optogenetic stimulation of GLP-1 terminals in the PVN. *Insert*, the expression of ChR2 in NTS and the location of the implanted optic fiber in the PVN. **N**, Food intake is significantly decreased after exposure to blue light in AAV-DIO-ChR2-YFP infected *Gcg-Cre* mice when compared to the control group (AAV-DIO-GFP infected *Gcg-Cre* mice), and in Gcg-Vglut2 KO animals. Mice were fed with ~0.5g food overnight. **O**, Food intake is significantly increased after exposure to 530nm light in AAV-DIO-Arch3.0-YFP infected *Gcg-Cre* mice when compared to the control group expressing YFP (1.2–1.5g food fed overnight). **P**, Experimental paradigm for optogenetic stimulation of GLP-1 terminals in the PVN and chemogenetic inhibition of CRH neurons. **Q**, Food intake suppression induced by 470nm light is completely abolished by silencing CRH neurons chemogenetically (0.5g food fed overnight). Food intake amounts were 0.5±0.072 g vs 0.84±0.084 g (n=9). See also Figure S1&2. Data are presented as Mean ± S.E.M, and n numbers are indicated in bars. * P<0.05; *** P<0.001, Student t-test (C and D); one-way ANOVA, posthoc Bonferroni test (N, O); paired student t-test (Q).

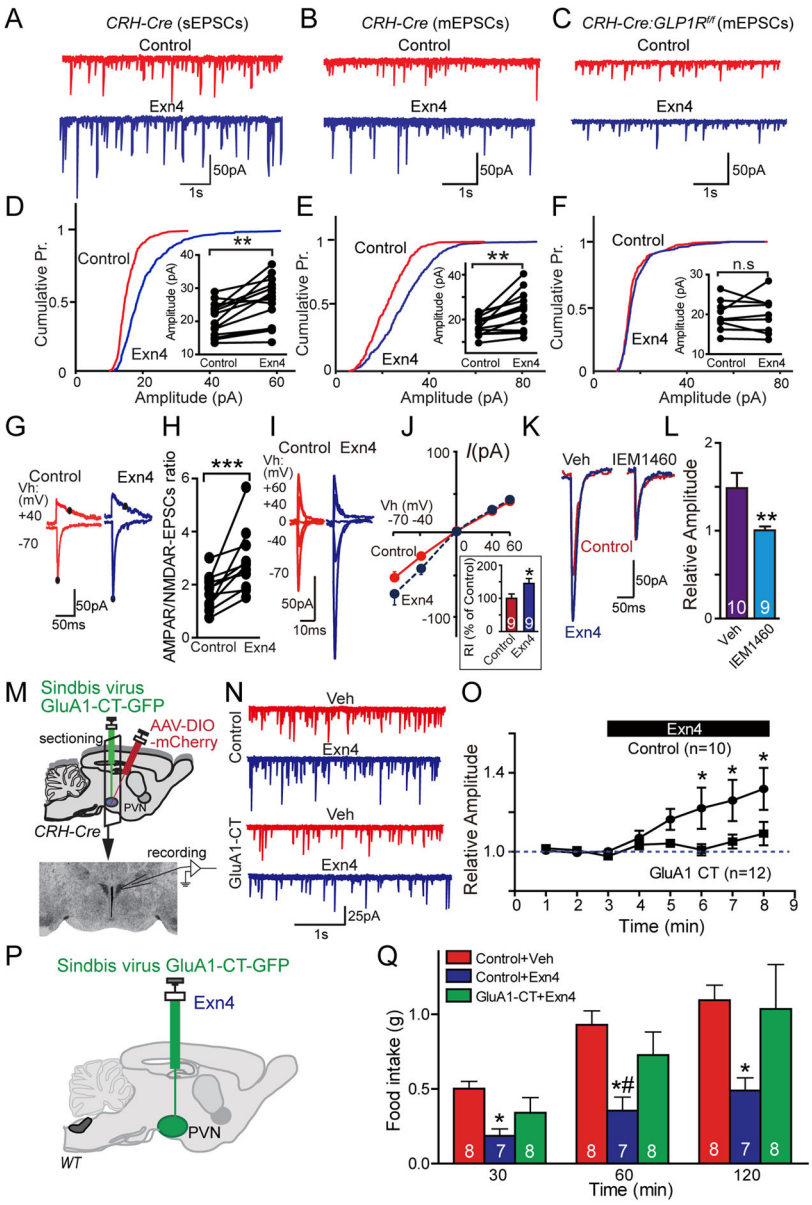

Figure 2. GLP-1 signaling augments excitatory synaptic drive to PVN neurons

A&B, Representative traces of sEPSCs (A) and mEPSCs (B) in PVN CRH neurons before and after the application of Exn4 in *CRH-Cre* animals. CRH neurons were identified by Cre-dependent expression of mCherry. **C,** Representative traces of mEPSCs in PVN CRH neurons in CRH-GLP-1R KO animals. **D&E,** Cumulative amplitude probability plots of sEPSCs (D) and mEPSCs (E) in typical PVN CRH neurons before and after Exn4 application. *Inset in D:* pooled data. n=14/8,cells/animals; P<0.001 (K–S test) for cumulative probability and **P<0.01, paired t-test, for sEPSC amplitude s(21.42±1.32 vs 26.84±1.91 pA). *Insert in* E: pooled data. n=14/8, cells/animals; **P<0.001 for cumulative probability (K–S test) and **P<0.01, paired t-test, for amplitude (17.21±1.06 vs 23.74±2.24 pA); **F**, No effects of Exn4 on mEPSCs in CRH-GLP-1R KO neurons (20.21078±1.27 vs 20.39±1.55 pA, n=9/5. **G,** Representative traces of evoked EPSCs in the presence of PTX in PVN CRH

neurons. *Black Dots* indicate that AMPAR-EPSC was measured at the peak at a holding potential of -70 mV and NMDAR-EPSC was measured 50 ms after the stimulation at a holding potential of +40 mV. **H,** Exn4 significantly increases AMPAR / NMDAR EPSC ratio in CRH neurons (1.75±0.196 vs 2.88±0.351, control vs. Exn4). n=11/9, cells/animals; *** P<0.001, paired t-test; I**,** Representative AMPAR-EPSCs isolated by pharmacological blockers (PTX and D-APV) at holding potential indicated, with 100μM spermine in the internal solution. **J,** I–V relationship of evoked EPSCs and holding potentials. *Insert*, rectification indices (defined by EPSC amplitude at −70 mV/ amplitude at +40 mV), n=9/6 cells/animals; data are presented as Mean ± SEM, * P<0.05, paired t-test; **K,** Representative traces of AMPAR- EPSCs with or without IEM1460, a specific GluA2 lacking AMPA receptor blocker, before and after application of Exn4. **L,** Pooled data showing that Exn4 induced facilitation of EPSC can be completely blocked by IEM1460, n=10/4 for control, and 9/4, cells/animals for IEM1460 group, student t-test, ** P<0.01; **M,** Experimental paradigm for manipulating AMPA receptor trafficking using sindbis viral mediated expression of GluA1-C terminal fragment (CT). **N,** Representative traces of mEPSCs before and after application of Exn4 in PVN CRH neurons expressing GFP only or GluA1-CT-GFP. **O,** Pooled data showing that expression of GluA1-CT-GFP in CRH neurons blocked Exn4 induced facilitation of mEPSCs. Data are presented as Mean ± S.E.M. n=10/8 and 12/8, cells/animals, for control and GluA1-CT groups, respectively; * P<0.05, repeated measures ANOVA, posthoc Bonferroni t-test. **P**, Experimental paradigm for Exn4 effect on food intake in GluA1-CT-GFP expressing animals. **Q,** Exn4 injection in PVN suppresses food intake, which can be blunted by expressing GluA1-CT in PVN neurons (repeated measures ANOVA, group effect: P=0.01; posthoc t-test P<0.01), * when comparing control vehicle group with control Exn4 group at each time point, P=0.02, # when comparing control Exn4 group with GluA1-CT Exn4 group at 60min. Data are presented as Mean ± S.E.M., n numbers are indicated in bars. See also Figure S2&3.

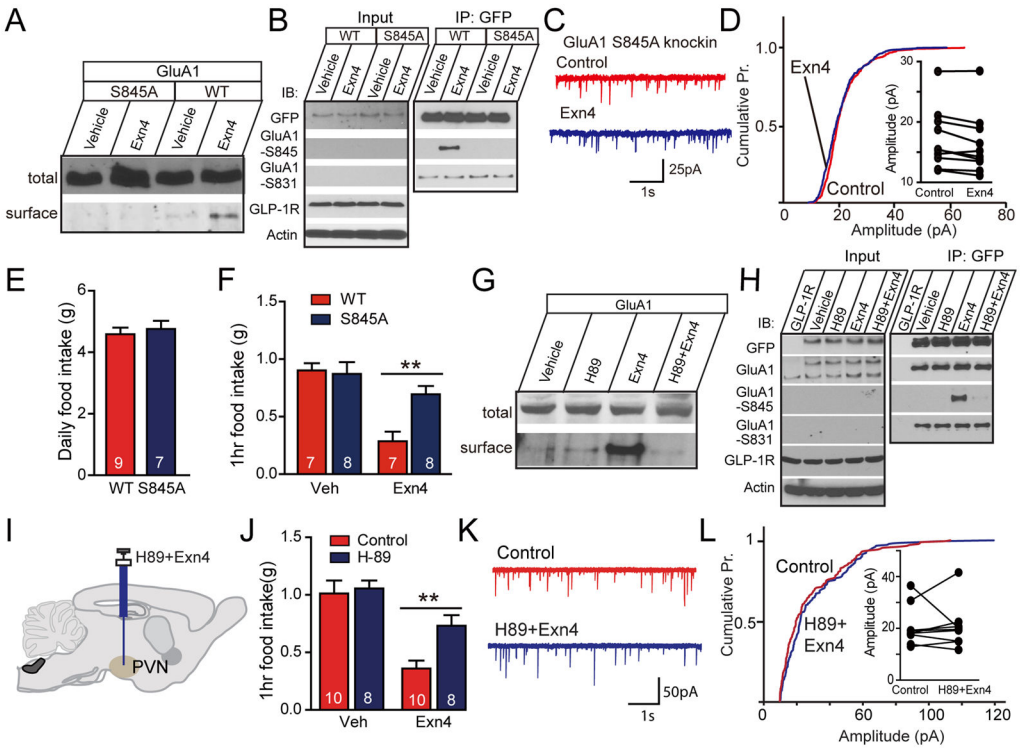

Figure 3. GLP-1R activation promotes GluA1 membrane trafficking by phosphorylation of S845

A, Biotinylated membrane protein assay shows increased membrane GluA1 in Exn4 treated N2a cells, which can be completely abolished by S845A substitution on GluA1.**B,** GFP-immunoprecipitation (IP) shows increased S845 phosphorylation of GluA1 after Exn4 treatment which can be diminished by the S845A mutation. IB: immunoblotting. **C,** Representative traces of mEPSCs in PVN CRH neurons before and after the application of Exn4 in S845A mutant animals. **D,** Cumulative probability plots of the amplitudes of sEPSCs. *Insert,* pooled data. n=9/4; The sEPSC amplitudes are 17.22±1.58 vs. 16.35±1.61pA in control vs. Exn4. **E**, No difference in daily food intake between wild type and S845A mutant mice was observed. **F.** Significant difference in food intake after application of Exn4 between WT and S845A mice within 1 hour of re-feeding post fasting. **G,**Biotinylated membrane protein assay shows increased membrane GluA1 in Exn4 treated cells, which can be blocked by PKA inhibitor-H89. **H,** Exn4 induced insertion of surface GluA1 can be completely abolished by mutation of Ser845 to Ala845 in the GluA1 subunit. **I,** Experimental paradigm for manipulating the PKA pathway in PVN by injecting H-89. **J,** Co-infusion of CNO and H89 partially blocked CNO induced suppression of food intake within 1 hour of re-feeding post-fasting. **K,** Representative traces of mEPSCs in vehicle or with H89+Exn4. **L,** Cumulative distribution of mEPSC amplitudes. *Insert*: pooled data. The average amplitudes of mEPSCs are 20.69±2.59 vs 20.62±2.86, in control vs. H89+Exn4 groups, respectively. n=9/5, cells/animals. Data are presented as Mean ± S.E.M. or absolute values, **P<0.01, n numbers are indicated in bars or as indicated. K–S tests, and paired t-tests were employed for D and L cumulative curve and inserted dot plots; one-way ANOVA was used for E, F and J. See also Figure S4.

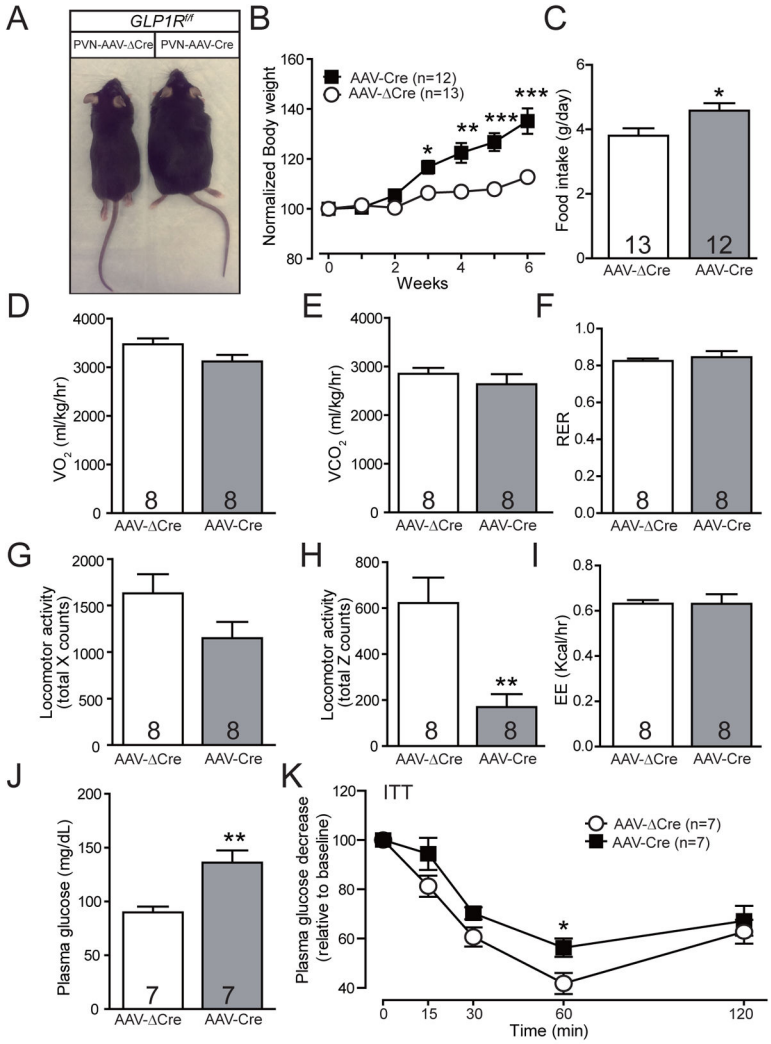

Figure 4. Depletion of GLP-1R in PVN causes obesity

A, GLP-1 PVN neuronal specific knockout of GLP-1R (*GLP-1R*$^{f/f}$ with AAV-Cre) caused body weight gain. **B,** Quantitation of body weight gain after depletion of GLP-1R in PVN. **C**, GLP-1R depleted mice have higher daily food intake when compared to control animals. **D**, O_2 consumption is unchanged; **E**, the elimination of CO_2 is also unaltered. **F**, respiration exchange rate is not changed by depletion of GLP-1R. **G**, locomotor activity in the X-axis is not different between the two groups. **H**, but PVN GLP-1R knockout mice showed significantly decreased Z-axis activity. **I**, No difference in energy expenditure between the two groups was observed; **J**, PVN GLP-1R knockout mice show higher fasting glucose. **K**, and impaired insulin sensitivity. Data are presented as Mean ± S.E.M. and n numbers are indicated in each plots; * P<0.05; **P<0.01;***P<0.001. Specific statistical analyses are: for B and K, repeat measurement group effect: P<0.01, post-hoc tests were used; student t-tests are applied to D–J.

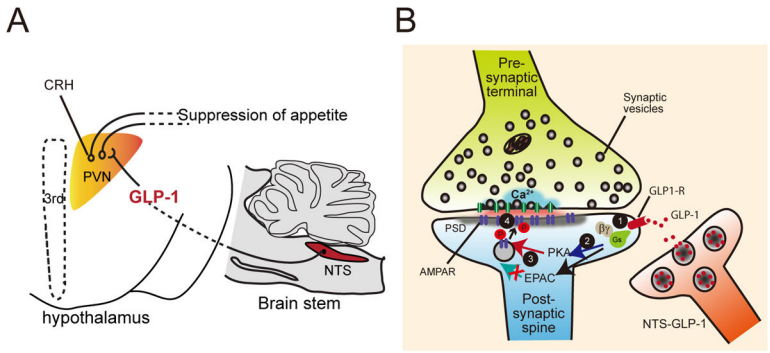

Figure 5. NTS-to-PVH GLP-1 signaling pathway regulates food intake

A, NTS→PVN GLP-1 signaling affects food intake. **B**, GLP-1 binding to GLP1-R (1) and activation of the PKA pathway (2), followed by phosphorylation of S845 of the AMPA receptor subunit-GluR1 (3), thus promoting GluR1 membrane trafficking and increased post-synaptic plasticity of CRH neurons which results in excitatory effects on post-synaptic neurons (4).